Available online at www.sciencedirect.com

ScienceDirect

Procedia Manufacturing 48 (2020) 159–164

Procedia MANUFACTURING

www.elsevier.com/locate/procedia

48th SME North American Manufacturing Research Conference, NAMRC 48 (Cancelled due to COVID-19)

Preliminary experimental analysis of the surface topography formation during laser polishing H13 tooling steel using statistical characteristics of the surface amplitude distribution

Evgueni V. Bordatchev[a,b,*,‡], Srdjan J. Cvijanovic[b,a,‡], Remus O. Tutunea-Fatan[b,a,*]

[a]National Research Council of Canada, 800 Collip Circle, London, ON, N6G 4X8 Canada
[b]Department of Mechanical and Materials Engineering, Western University, London, ON, N6A 5B9 Canada

* Corresponding authors. Tel.: +1-226-688-5604; fax: +1-519-430-7064. *E-mail address:* evgueni.bordatchev@nrc-cnrc.gc.ca, rtutunea@eng.uwo.ca

Abstract

Surface finish is one of the most important quality characteristics of fabricated components. To complement that, laser polishing (LP) is one of the advanced manufacturing surface finishing techniques that has been recently developed and successfully employed for improving surface quality without deteriorating the overall structural form through surface smoothing by melting and redistributing a thin layer of molten material. This paper proposes a statistical digital twin of the LP process and demonstrates the applicability of amplitude distribution statistical characteristics in the experimental analysis of surface topography formation during LP process. Initially, the thermodynamic transformation of the initial surface topography is considered by means of technical cybernetics and machine learning approaches to describe two of the most critical LP process components, namely: thermodynamic melting and solidification of both solid material and surface topography. To exemplify the effective application of statistical amplitude distribution characteristics, LP experiments were conducted with two different laser powers (25 W and 100 W) on flat and ground initial surfaces and resulting surface topographies were measured. Several amplitude distribution characteristics, such as roughness average value, averaged transverse profile as a W-shape, averaged transverse roughness profile, and probability distribution function were calculated. After that, actual molten material area, volume redistribution and final surface quality were comparatively analyzed. It was shown that the proportion between two components of the LP thermodynamic transformation and surface topography is critically dependent on laser power. As such, during low-power conditions (< 25 W), surface quality is predominantly determined by the thermodynamic transformation of initial surface topography and therefore only this component can be used for statistically reliable LP process modelling and digital identification. In summary, amplitude distribution characteristics have several advantages in building a comprehensive understanding of the molten material redistributing along and across LP line.

Keywords: Type your keywords here, separated by semicolons ;

1. Introduction

According to industry axioms, functional components fabricated from various ferrous and non-ferrous materials require superior surface qualities. Laser polishing (LP) is an advanced surface finishing technique that has been continuously developed and enhanced over the past two decades [1-6]. LP is productive to the level of several seconds/cm^2 and improves surface quality by smoothing, melting and redistributing a thin layer of molten material. This happens without affecting the form precision and accuracy of the polished component. LP does not involve material removal or addition. LP does not require a physical contact between tool and workpiece and is typically regarded as an environmentally friendly process. However, LP performance depends on the physical-mechanical properties of the workpiece material, LP process parameters as related to the delivery of the laser energy (optics and motion), complex thermodynamics of laser-material interactions, as well as several other process/system details.

10.1016/j.promfg.2020.05.033

The main functional goal of LP is related to the flattening of the initial surface to a desired polished topography. During LP process, CNC-controlled laser beam travels over the surface and produces a localized pool of the molten material. Molten pool travels along with the laser spot and because of that, a thin top layer of material is continuously melting while being redistributed. The newly formed surface topography rapidly solidifies improving surface quality up to 95% [6].

The current study plans to demonstrate that the resulting quality of the LP surface is affected by two interrelated thermodynamic processes induced by the moving laser source, namely melting, redistribution and solidification of both solid body and surface topography. For this purpose, a statistical twin of the LP process was developed, and several LP experiments were performed on initially flat and ground surfaces. Following that, amplitude distribution statistical characteristics were calculated and analyzed to identify contributions from laser melting of solid body and surface topography.

2. Laser polishing process and its statistical digital twin

As shown in the past [7], final LP surface topography is comprised of two distorted material components: laser modification of both solid body and top surface topography. In addition to these two components, LP surface incorporates two distinct classes of surface structures: i) ripples and undercuts produced by the dynamics of the melt/solidification front, and ii) bulges, step structures, and martensite needles produced by plastic deformation and changes in the microstructure.

The two material components affected by laser energy can be regarded as the result of two LP regimes that are essentially dependent on the thickness of the molten layer, namely: shallow surface melting (SSM) and surface over melting (SOM) [8]. SSM regime was defined as having a molten layer thickness smaller than peak-to-valley distance such that molten peaks will flow down to valleys under the action of the capillary pressure. SSM can be understood as a capillary regime [5] in which dominating surface tension and viscosity smoothens high spatial frequencies of the surface topography. By contrast, SOM regime is present when a molten layer thickness is greater than the peak-to-valley distance. The presence of SOM implies that the initial surface topography will disappear completely. The two regimes coexist during LP but they are present in different ratios [5, 6, 8] and the dominating one will essentially define the mechanism underlying the final surface quality.

Preliminary statistical modelling, identification and spectral analysis of the laser micropolishing (LμP) process were previously conducted. According to [9], LμP can be considered as a single-input/ single-output dynamic system. In a different approach, LP process can also be regarded as a thermodynamic formation of the polished surface topography $h_{LP}(x,y)$. Previous LP studies [5, 6, 8, 10] have demonstrated that the thermodynamics of the laser-material interactions simultaneously affects both solid body and initial surface topography. This enables the modelling of LP process from two perspectives: i) thermodynamic distortion of the flat solid body, and ii) laser smoothing of the initial surface topography $h_{ini}(x,y)$ into $h_{LP}(x,y)$. Therefore, the digital twin of the LP process can be defined as a thermodynamic transfer function $W_{LP}(\cdot)$ having $h_{orig}(x,y)$ as a combined two-fold input, namely solid material and its surface topography. In this case, topography $h_{LP}(x,y)$ is considered as an output that combines the two aspects mentioned above (thermodynamic and statistical) that would concurrently roughen and polish $h_{orig}(x,y)$. The superposition of these two simultaneous processes will define the final quality of the surface. As such, LP parameter optimization will consist in the minimization of the thermodynamic material distortion as well as the maximization of laser smoothing effect as applied on the initial surface topography $h_{ini}(x,y)$. A schematic representation of the statistical digital twin of LP is shown in Fig. 1.

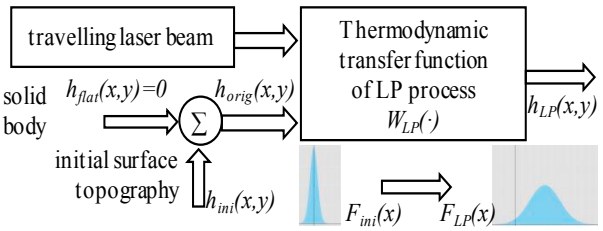

Fig. 1. Statistical digital twin of the LP process.

$$S_{LP}(\omega) = S_{flat}(\omega)\left|W_{LP}(j\omega)\right|^2 + S_{ini}(\omega)\left|W_{LP}(j\omega)\right|^2 \quad (1)$$

where $W_{LP}(j\omega)$ is the transfer function of LP process; $S_{flat}(\omega)$, $S_{ini}(\omega)$ and $S_{LP}(\omega)$ are the autospectrums of flat, initial and polished surface profiles, respectively; ω is the spatial frequency, and $j = \sqrt{-1}$ is the imaginary unit. This technical cybernetic description allows modelling and understanding LP process as a linear thermodynamic system transforming statistical characteristics of initial into LP surface (e.g. probability density functions $F(x)$) and laser beam interactions with flat solid body and non-uniform initial surface.

3. LP system and surface analysis methodology

LP experiments with identical process parameters are to be applied on two different initial surface (flat and ground) with an underlying assumption that the distortion of the flat surface topography $h_{ini}(x,y)$ into $h_{LP}(x,y)$ underlies the thermodynamic component of surface formation $W_{LP}(\cdot)$, whereas the redistribution of amplitudes of $h_{ini}(x,y)$ into $h_{LP}(x,y)$ will drive the statistical component of the LP process. Initial surface of a flat sample with S_a = 0.025 - 0.033 μm was obtained via single point diamond cutting. Ground initial surface topography incorporates a variety of spatial frequencies having a profile average roughness R_a = 0.75…0.98 μm.

The LP system shown in Fig. 2a is a complex opto-electro-mechanical CNC-controlled system and consisting of a high-precision 3-axis motion system and a 1070 nm, 500 W continuous wave (cw) laser from IPG Photonics (model YLR-500). The motion system is controlled by a CNC Aerotech controller with a positional resolution of 0.1 μm. In addition, to allow high speed 2D scanning within 100 x 100 mm working

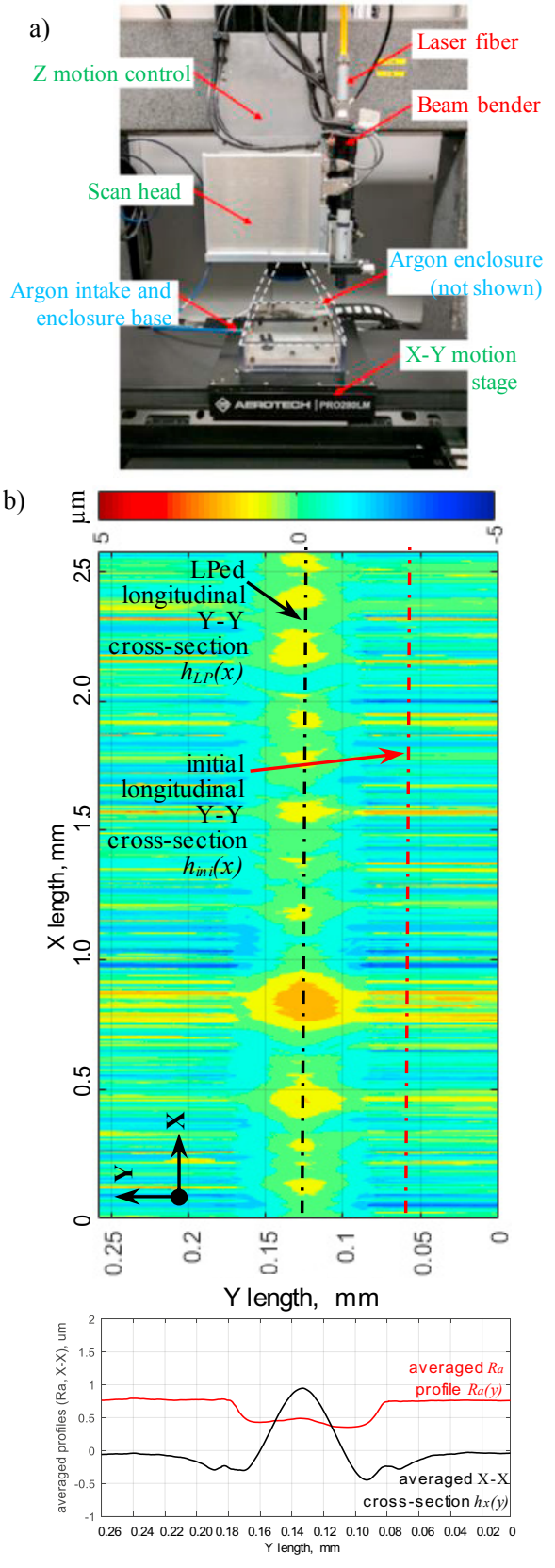

Fig. 2. a) LP system and b) surface analysis methodology.

envelope, the laser beam was directed to a 2-axis galvanometric scanning head, manufactured by ScanLab and with an *f*-theta objective having a focal length of 160 mm.

Two sets of LP experiments with the same parameters were performed by varying laser power and travel speed (Fig. 3) in order to investigate two different LP regimes (SSM *vs* SOM) as well as contributions of melting solid body and initial surface topography on the final LP topography.

The analysis of the surface topography presented in Fig. 2b involved the following steps: a) measure initial surface geometry $h_{ini}(x,y)$ between alignment marks, b) perform LP experiments on the previously measured initial surface, c) measure LP surface geometry $h_{LP}(x,y)$, and d) calculate statistical characteristics of amplitude distribution for both $h_{ini}(x,y)$ and $h_{LP}(x,y)$, a process to be followed by their comparison. The sample surfaces before and after LP experiments were measured using a WYKO NT1100 white light interferometer having an 1 Å height measurement resolution and 0.258 µm/pixel resolution. An autostitching technique was used to expand the limited field of view.

Furthermore, measured and digitized $h_{ini}(x)$ and $h_{LP}(x)$ were used for calculating specific statistical parameters and characteristics of the transverse profile amplitude distribution along Y axis, such as roughness average value R_a, averaged transverse X-X cross-section $h_x(y)$, averaged roughness transverse R_a profile $R_a(y)$, density histogram $p_x(y)$, and material ratio function $MR(y)$.

4. Effect of the laser power on flat and ground surfaces

The effect of laser power on surface topography formation and its thermodynamic and statistical components was studied by comparing initial and LP longitudinal Y-Y cross-sections $h_{ini}(x)$ and $h_{LP}(x)$ of ground and flat samples with different LP powers (25 W and 100 W). The post-polished surface topography in Fig. 4 suggests clear differences between initial and LP profiles of ground and flat surfaces. Two main observations can made based on the results presented in Fig. 4:

- LP with 25 W of applied power is associated with SSM, capillary and laser micropolishing regimes as LP process acts as a moving average of the ground surface topography. More specifically, LP process melts peaks to fill cavities. This will consequently smoothen the surface profile and reduce initial surface roughness since R_a drops from 0.746 um to 0.488 um for the ground surface (see Fig. 4a). This regime will minimally affect the surface waviness, and it is characterized by a very low molten depth that cannot be measured accurately. SSM is associated with a strong statistical correlation between initial and LP surfaces and very high damping of profile amplitudes in the high areal frequency range. This represents the statistical component of the transfer function of the LP process $W_{LP}(\cdot)$.
- LP with 25 W of applied laser power worsens the quality of the initially flat surface. More specifically, its R_a increased by 300% from 0.033 µm to 0.099 µm (see Fig. 4b). However, cw LP elevates the mean value of the LP longitudinal Y-Y cross-sections $h_{LP}(x)$ thus creating a

so-called “surface bulging” phenomenon. This mean value is also laser power dependent since it increased from 0 to 0.393 µm for ground surface and to 0.261 µm for flat solid body, respectively. The bulging effect can be seen as a compound/composite effect since its characteristic bulging height was determined by upward movements of the bulk material as well as contributions from melting peaks.

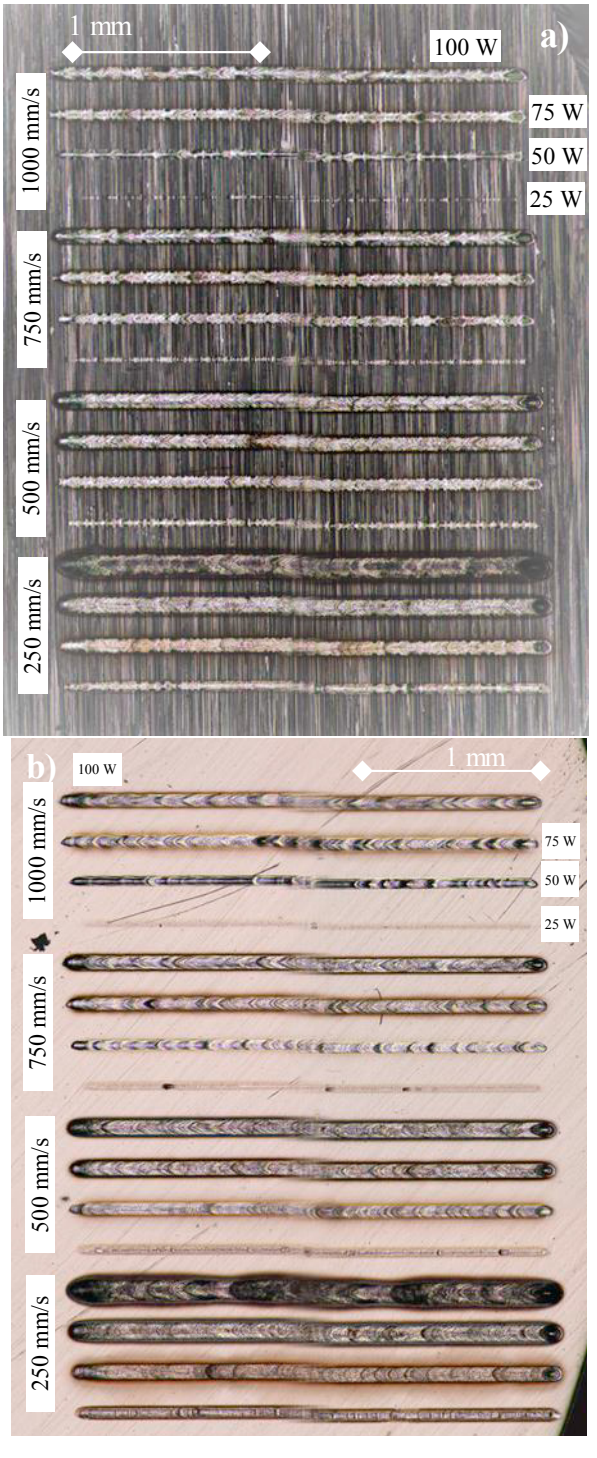

Fig. 3. LP samples with a) ground initial surface and b) flat initial surface.

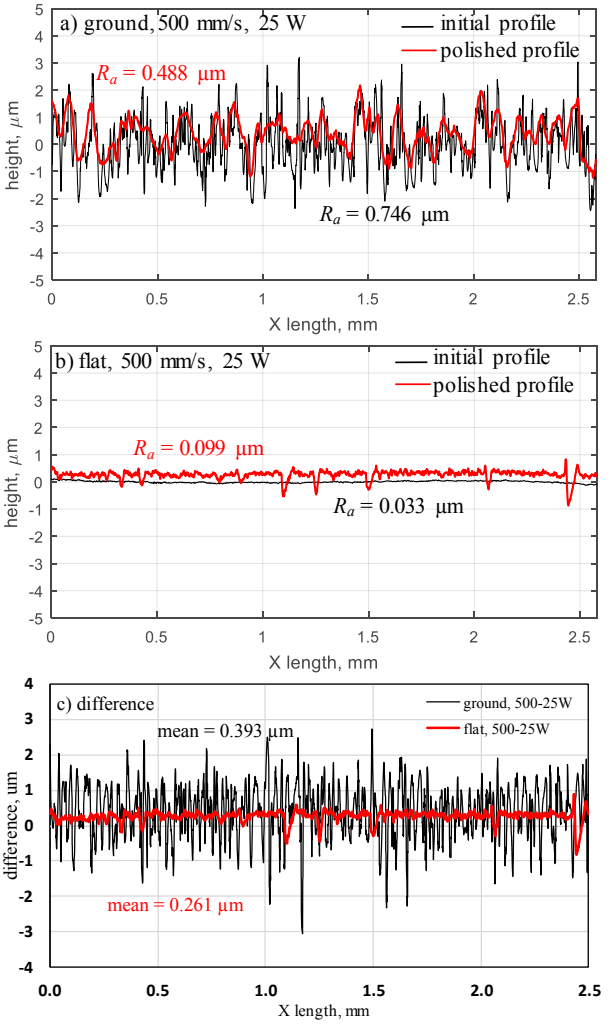

Fig. 4. Effect of 25 W laser power on ground and flat surface topography: a) initial and LP longitudinal Y-Y cross-sections of ground sample, b) initial and LP Y-Y cross-sections of flat sample, and c) difference between initial and LP Y-Y cross-sections of ground and flat surfaces.

When LP is performed at 100 W of applied laser power (see Fig. 5), SOM regime and thermo-capillary effects are present. In this case, LP process acts as an amplitude modulator of the ground surface topography. The initially flat surface topography was completely eroded since R_a increased from 0.033 µm to 0.391 µm. The amplitude distribution of frequency components has also changed significantly. As expected [9, 10], the bulging effect was more prominent for 100 W, rather than 25 W of power. Unlike in the low power case, R_a for LP ground and flat samples are comparable: 0.510 µm *vs* 0.391 µm (see Figs. 5a and 5b), thus suggesting that molten material from bulk solid body and surface topography are significantly blending with each other. Although R_a has still improved considerably from 0.801 µm to 0.510 µm (see Fig. 5a), the thermodynamic mechanism involved in LP surface formation was completely different in a sense that this time, solid body elevation seems to play a predominant role on the overall process of bulge formation.

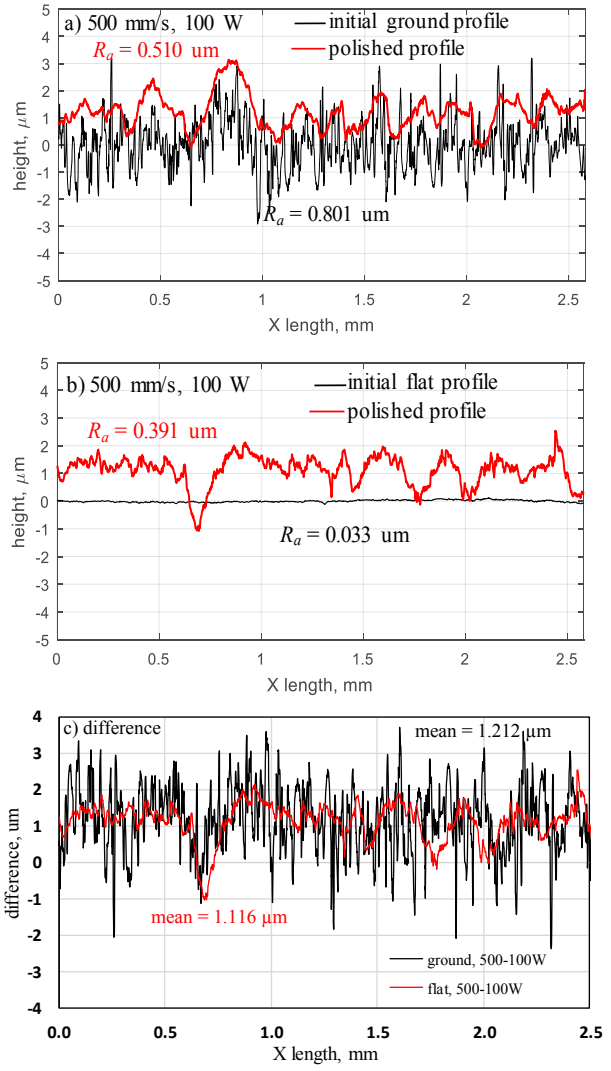

Fig. 5. Effect of 100 W laser power on surface topography: a) initial and LP longitudinal Y-Y cross-sections of ground sample, b) initial and LP Y-Y cross-sections of flat sample, and c) difference between initial and LP Y-Y cross-sections of ground and flat surfaces.

As a next step in the current analysis, the overall formation of LP line topography was analyzed in detail on both flat and ground surfaces polished by averaging transversal X-X cross-sections along laser travel trajectory (see Fig. 6). These cross-sections represent the result of the molten material redistribution during LP and overall form quality of the LP line. As it was shown before [9], typically, the averaged transversal X-X cross-section is characterized by a specific "W"-shape. The central bulge is always present after LP and its height increases with higher laser power levels: 0.383 μm for 25 W vs 0.947 μm for 100 W (ground sample case). The lateral pocket depths also increase from 0.096 μm for 25 W to 0.382 μm for 100 W. One other important characteristic of the averaged transversal X-X cross-section is an areal material distribution under the "W"-shape. This distribution consists of a centrally raised area (bulging) coupled with laterally lower regions (pocket).

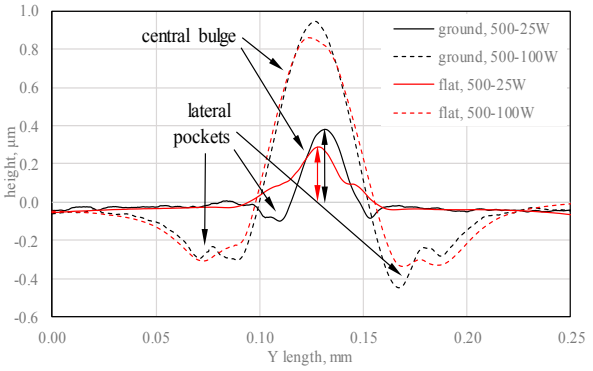

Fig. 6. Effect of the laser power on averaged transversal X-X cross-sections.

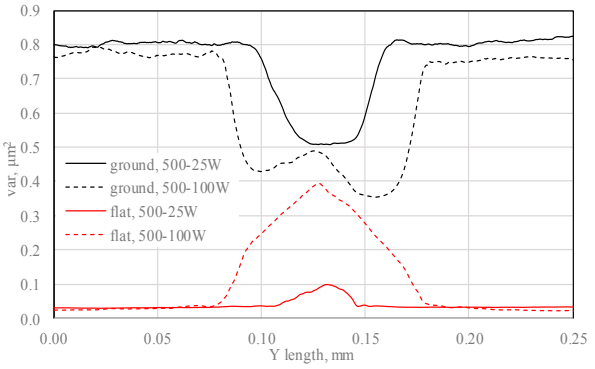

Fig. 7. R_a profiles for different laser powers (25 W and 100 W).

The direct comparison of $R_a(y)$ profiles on Fig. 7 indicates clearly that laser melting of solid body with 25 W does not significantly affect the surface quality of LP ground geometry while 100 W will significantly alter it. This implies that the ratio between the two components of the LP thermodynamic transformation is critically dependent on the applied laser power.

Additional aspects of the material redistribution during LP can be also explored using a classical probability density function $F(y)$ [11, 12] for analysis of surface topography amplitudes distributions. Experimental analysis and comparison of $F(y)$ for LP with 25 W and 100 W are shown in Fig. 8. For the initial flat surface, $F_{ini,flat}(y)$ is very similar to a Dirac delta function with a very sharp amplitude of 1. After applying 25 W LP to initial flat surface, $F_{ini,flat,25W}(y)$ becomes wider with reduced maximum amplitude. This describes the thermodynamic transformation of solid material, which increases average surface waviness and roughness and produces a bulging effect. $F_{ini,ground,25W}(y)$ for LP with 25 W has an opposite signature, where Gaussian distribution of the initial ground surface is transformed into a narrowed shape with higher maximum amplitude. This represents the combination of both thermodynamic transformations during LP – a) bulging induced by melting-and-solidification of solid material and resulted in increasing the waviness and b) surface smoothing induced by melting-and-solidification of initial surface topography and resulted in surface quality improvement.

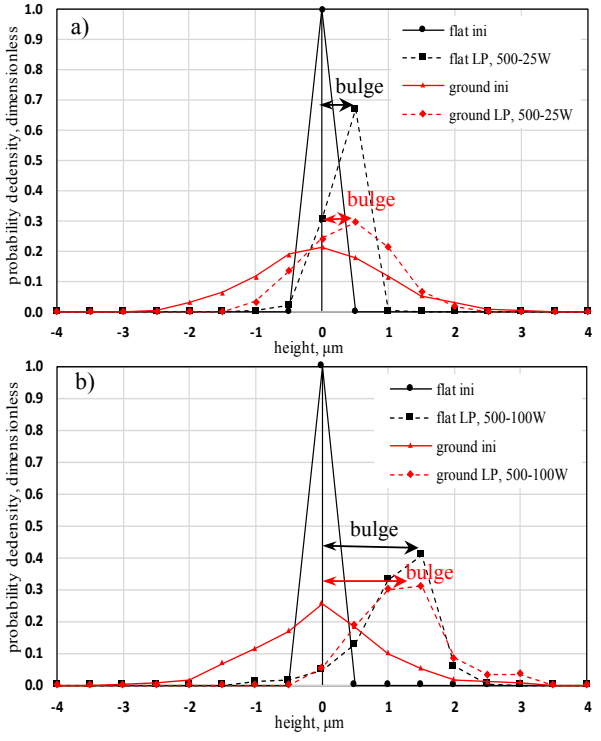

Fig. 8. Probability density histograms for: a) 25 W laser power and b) 100 W laser powers

Same observations mentioned above can be applied for LP with 100 W however producing bigger bulging effect, larger amplitude of the surface waviness, and in overall less surface quality. This is because LP simultaneously and continuously melts, redistributes and resolidifies solid material within a laser-material interaction volume.

5. Summary and conclusions

The present study advocates towards the use of advanced statistical amplitude distribution characteristics in the analysis of the LP process. In this context, the emphasis was placed on the experimental characterization of two major components of thermodynamic transformation of the initial surface. The current body of work warrants several important conclusions:

- LP is a complex physical-thermo-dynamic process, with two major thermodynamic components: i) melting, redistribution and solidification of both solid material and ii) initial surface topography.
- Concept of the statistical digital twin of the LP process has been introduced and explored in this study as the transformation of the statistical characteristics of the initial and LP surfaces, such as a probability density function.
- Thermodynamic transformation of solid material generally leads to bulging and increased surface waviness.
- Thermodynamic transformation of the initial surface generally leads to smoothing as well as desirable results in surface quality improvement.
- Final LP surface is formed by a complex, volumetric, and non-linear combination of the two aforementioned components. Their superposition will define the final surface quality.
- The two thermodynamic components are critically dependent on the applied laser power. More specifically, low power conditions imply that surface quality is predominantly formed by the thermodynamic transformation of initial surface topography and therefore only this component can be used for statistically reliable LP process modelling and its digital identification.
- A superior understanding of all aspects associated with thermodynamic melting, redistribution and solidification of workpiece material requires further in-depth analysis and extensive modelling and experimental investigations.
- Future extension of this work will focus on the variation of other process parameters (such as travel speed) in an attempt to further understand the mechanisms underlying the LP process.

Acknowledgements

This study is the result of collaboration between the National Research Council of Canada (London, Ontario) and Western University (London, Ontario). Partial financial support was also provided by the Natural Sciences and Engineering Research Council (NSERC) of Canada.

⁑ These authors contributed equally to this work

References

[1] Willenborg E. Polieren von werkzeugstählen mit laserstrahlung, Dissertation RWTH Aachen, Shaker Verlag Aachen; 2006. 153 p.
[2] Willenborg E. Polishing with laser radiation. In: Poprawe R, editor: Tailored Light 2: Laser Allication Technology; 2011. pp. 196-202.
[3] Temmler A, Willenborg E, Wissenbach K. Laser polishing. Proceedings of SPIE 2012; vol. 8243, paper 82430W, 13 p.
[4] Perry TL, Werschoeller D, Li X, Pfefferkorn FE. Duffie NA. Pulsed laser polishing of micro-milled Ti6Al4V samples. Journal of Manufacturing Processes 2009; 11(2): 74-81.
[5] Pfefferkorn FE, Duffie NA, Li X, Vadali M, Ma C. Improving surface finish in pulsed laser micro polishing using thermocapillary flow. CIRP Annals – Manuf Tech 2013; 62:203-6.
[6] Bordatchev EV, Hafiz AMK, Tutunea-Fatan OR. Performance of laser polishing in finishing of metallic surfaces. International Journal of Advanced Manufacturing Technologies 2014; 73:35–52.
[7] Nusser C, Kumstel J, Kiedrowski T, Diatlov A, and Willenborg E. Process- and material-induced surface structures during laser polishing. Advanced Engineering Materials 2015; 3:268-77.
[8] Ukar E, Lamikiz A, López de Lacalle LN, del Pozo D, Arana JL. Laser polishing of tool steel with CO2 laser and high-power diode laser. Int'l Journal of Advanced Manufacturing Technologies 2010; 50:115–25.
[9] Chow MTC, Bordatchev EV, Knopf GK. Impact of initial surface parameters on the final quality of laser micro-polished surfaces. Proceedings of SPIE 2012; vol. 8248, paper 824809, 10 p.
[10] Bordatchev EV, Cvijanovic SJ, Tutunea-Fatan O R. Effect of initial surface topography during laser polishing process: Statistical analysis. Procedia Manufacturing 2019; 34:269–74.
[11] Whitehouse DJ. Handbook of surface and nanometrology. 2nd ed. CRC Press; 2011. 955 p.
[12] Bendat JS, Piersol AG. Engineering applications of correlation and spectral analysis. New York: John Wiley & Sons; 1993.